IOSR Journal of Mechanical and Civil Engineering (IOSR-JMCE)
e-ISSN: 2278-1684,p-ISSN: 2320-334X
PP. 30-36
www.iosrjournals.org

Joining processes of Aluminium Alloy and Stainless Steel material using tungsten inert gas welding and Brazing.

K.Nageswara Rao[1] Dr.B.V.R. Ravi Kumar[2] Dr.M.T.Naik[3]

Associate Professor
St.Martin's Engineering College
Secundrabad.

Professor & Principal
NS RAJU Institue of Technology
Visakhapatnam.

Professor
JNTUH College of Engineering
Hyderabad

ABSTRACT:- *Different metals tungsten idle gas butt welding–brazing between 5A06 aluminum compound and SUS321 stainless steel might have been conveyed crazy utilizing Al–Cu6 filler metal Furthermore non-corrosive flux. A thin inter-metallic compound layer need structured done welded seam/steel interface and the Average thickness of the entirety layer will be 3–5 µm, which will be under the limit of 10 µm. The inter-metallic compound layer comprises for Fe_4Al_{13} period What's more in the base Sn stores in the liquid flux layer and diffuses under steel grid to structure the grain limit filter layer, which is the feeble zone of the butt joint. Those Normal micro hardness of the layer is 644. 7 HV, compared for 104. 5 HV done welded crease Also 200 HV over steel grid. Those rigidity for butt joint achieves 172. 5 MPa and the split initiates starting with the IMC layer at the base of the joint Also infers under welded crease In those upper and only those joint. Those display joint in this investigation need larger amount over the individuals for covered layer.*

KEYWORDS:- *Brazing, TIG, Butt welding, Aluminum alloy, Stainless steel.*

I. Introduction:-

Against the background of the required weight reduction in transportation through lightweight construction, the application of hybrid structures between aluminum alloy and steel has a high technical and economical potential [1,2]. However, joining of alu- minum alloy and steel has great difficulty by fusion welding since large number of brittle intermetallic compounds (IMCs) are formed in the joint. Although solid-state welding can be used to join the dissimilar metals by controlling the IMC layer's formation within a few micrometers [3–5], the joint's shape and size are extremely restricted by the welding equipment's capacity. Nowadays, tung- sten inert gas (TIG) welding–brazing offers a great potential for aluminum alloy and steel joining. In this process, the sheets and fil- ler metal are heated or melted by TIG arc heat, and the joint has a dual characteristics: in aluminum alloy side it is a welding joint, while in steel side it is a brazing joint [6–8].

However, in the dynamic heating process, the heating tempera- ture changes very quickly and the reaction time between the liquid filler metal and solid steel is rather short so that it is more difficult to control the IMC layer's growth, predominantly in its thickness and microstructures. Most of past reports about laser brazing and arc brazing of aluminum alloy and steel [9–11] indicated that coated layer on the steel surface, such as Zn or Al layer, could improve the filler metal's wetting and inhibit the IMC layer's growth. And it was recognized that Si additions in the filler metals effectively control the growth of the Al–Fe IMC layer by replacing Al–Fe binary phases with Al–Fe–Si ternary phases [10–12]. But in our previous study [13], it was found that Si addition in the filler metal had a limited effect on improving the IMC layer's crack resistance because Al–Fe–Si phase also presented a high brittle- ness. By now, there is no report about the effect of some other special additions, such as Cu or Mn elements on IMC layer's property in aluminum–steel joint.

In this study, dissimilar aluminum alloy–steel butt joint was made successfully by TIG welding–brazing using a modified non- corrosive flux and Al–Cu filler metal. The structures of the butt joint, especially the IMC layer, were characterized; the mechanical properties of the joint were evaluated and the cracking mechanics of the joint were discussed.

II. Materials And Methods:-

Materials used are 5A06 aluminum alloy and SUS321 austenite stainless steel plates in 3.0 mmthickness. The filler metal used is 2319 Al–Cu6 welding wire, with a diameter of 2.5 mm. TheChemical

compositions of base material and filler metal are shown in Tables 1–3. And the maincompositions of modified non-corrosive flux are Nocolok flux (KAlF4 and K3AlF6 eutectic), Zn and Sn metal powders, K2SiF6, etc.

All plates were cut into the size of 100 mm x 50 mm,and the surface was cleaned by abrasive paper and acetone before experiment. A single-V groovewas opened in the plates, with a bevel angle of 40 in steel side and 30 in aluminum alloy side.The flux suspension (flux powder dissolved in acetone) was smeared homogenously ina 0.2–0.5 mm thickness on the groove and on both front and back surfaces of the steel in10 mm width. Aluminum–steel butt TIG welding–brazing was carried out using CLOOS AC-TIG welding source. The schematic of the joining process is shown in Fig. 1. After welding,a typicalcross-section of the joint was cut and mounted in self-setting epoxy resin in an as-clamped condition.Then the samples were polished to a mirror-like surface aspect and etched with Keller'sreagentfor 3–5 s. Macrostructure of the joint was observed by optical metalloscope and microstructuresand compositions of IMCs were measured by scanning electron microscopy (SEM) andenergy dispersive spectrometer (EDS). The IMC layers were examined by micro X-ray diffraction(M-XRD) with Cu Ka radiation. And the mechanical properties of IMC layer weremeasuredby dynamic ultra-micro hardness tester and SEM in situ tensile tester.

Table 1:-

Chemical composition of 5A06								
Mn	Mg	Si	Fe	Cu	Zn	Be	Ti	Al
0.5–0.8	5.8–6.8	0.4	0.4	0.1	0.2	0.0001–0.0005	0.02–(	Bal.

Table 2:-Chemical composition of SUS321 stainless steel (wt.%).

C	Ni	Cr	M	Si	S	P	Ti	Fe
0.1	**8–**	**17–**	**2.0**	**1.0**	**0.0**	**0.03**	**0.1–**	**Bal.**

homogenously in a 0.2–0.5 mm thickness on the groove and on both front and back surfaces of the steel in 10 mm width. Aluminum–steel butt TIG welding–brazing was carried out using CLOOS AC-TIG welding source. The schematic of the joining process is shown in Fig. 1. After welding, a typical cross-section of the joint was cut and mounted in self-setting epoxy resin in an as-clamped condition. Then the samples were polished to a mirror-like surface aspect and etched with Keller's reagent for 3–5 s. Macrostructure of the joint was observed by optical metalloscope and microstructures and compositions of IMCs were measured by scanning electron microscopy (SEM) and energy dispersive spectrometer (EDS). The IMC layers were examined by micro X-ray diffraction (M-XRD) with Cu Ka radiation. And the mechanical properties of IMC layer were measured by dynamic ultra-micro hardness tester and SEM in situ tensile tester.

3. Results and discussion

3.1. Appearance and macrostructure

Fig. 2 shows the appearance of aluminum–steel butt joint made by TIG welding–brazing. The joint has a good front and back formation and no crack appears on the welded seam/steel interface and no undercut or incomplete fusion presents in aluminum alloy side. The flux slag carpets on the half surface of welded seam in steel side due to its low gravity and the residual flux deposits on the steel surface near the welded seam. Slag and residual flux on the surface can be removed easily by sanding the joint using the steel brush.Fig. 3 shows the typical cross-section of aluminum–steel butt joint. With the help of wetting action of the special flux layer, the Al–Cu filler metal spread fully on steel surface to form a sound joint. The joint has a typical welding–brazing dual characteristics: in aluminum alloy side, the base metal with low melting temperature is a welding joint, which mixes with the molten filler metal to form fusion area, while in steel side, the steel surface with a high melting point is a brazing joint, which reacts with the molten filler metal to form the brazing interface layer.

3.2. Microstructures and intermetallics

SEM images in different positions of the joint, plotted by dotted- line squares in Fig. 3, are shown in Fig. 4. A thin IMC layer has formed in welded seam/steel interface during the

welding process, as shown in Fig. 4a–d. The whole IMC layer presents different pat- terns at the different positions of the groove: at the top, the IMC

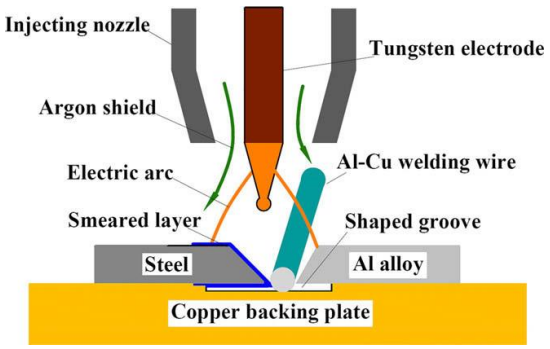

Fig. 1. Schematic of aluminum–steel butt TIG welding–brazing.

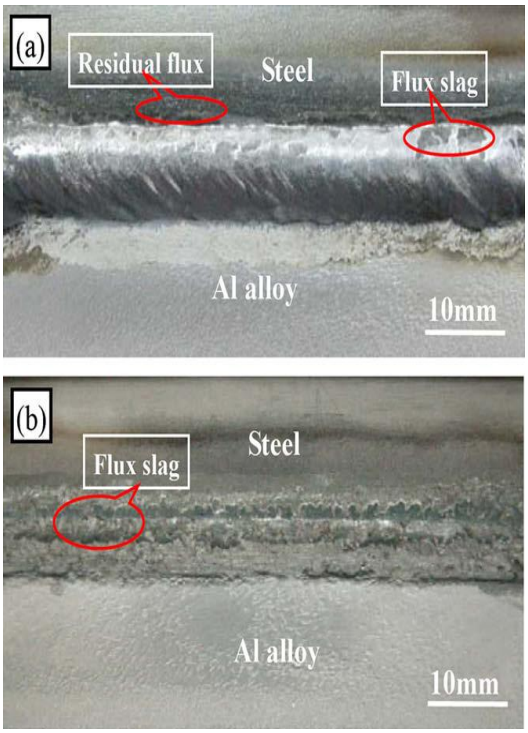

Fig. 2. Appearances of the aluminum–steel butt joint: (a) front formation and (b) back formation.

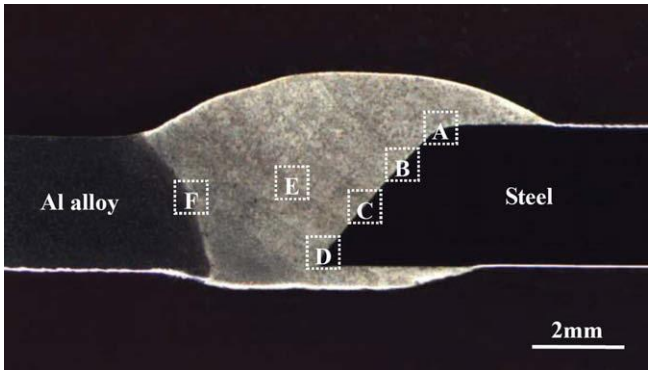

Fig. 3. Typical cross-section of the aluminum–steel butt joint with Al–Cu filler metal.

Table 3:- Chemical composition of 2319 filler metal (wt.%).

Cu	Mn	Mg	S	F	Zr	Z	Ti	V	A
5.8–	0.2–	0.2–	0	0	0.1–	0	0.1–	0.05	B

layer presents whisker shape oriented toward the welded seam; at the centre part, the IMC layer becomes compact lath-shaped structure; contrastively, at the bottom, the IMC layer presents loose lath-shaped and a grain boundary filter layer appears in steel side. According to the SEM features, in this layer, Sn and Zn elements from the molten flux diffuse into the steel grain boundary to form Fe–Sn and Fe–Zn filter layer. And the average thickness of the whole IMC layer is 3–5 μm, which is less than the limited value of 10 μm [14].

The welded seam, as shown in Fig. 4e, mainly consists of a-Al matrix and (α-Al + Al_2Cu eutectic) in the grain boundary. Due to the high cooling rate, α-Al in (α-Al + Al_2Cu eutectic) grows with α-Al matrix and only Al_2Cu remains in the grain boundary, which is called as the divorced eutectic. Fig. 3f shows the microstructure of the fusion area in aluminum alloy side. In the welding process, the α-Al matrix of Al–Mg base material is not melted, while the grain boundary is melted due to its low melting temperature. Hence the molten Al–Cu filler metal enters and reacts with Al–Mg molten metal to form network (α-Al + Al_2Cu + Al_2CuMg eutectic) structure. And some block high-temperature phases in the base materials remains in the fusion area.

Table 4:-EDS analysis results of ntermetallic hases in the joint (wt.%).

Poin	Al	Cu	Fe	Cr	Ni	Mn	M	Zn	Sn
A	59.	2.5	28.	5.6	2.8	1.3	–	–	–
B	–	0.8	59.	15.	2.5	1.6	–	3.2	17.5
C	58.	38.	1.4	0.4	0.9	0.5	–	–	–
D	63.	25.	0.6	0.4	0.8	0.4	8.6	–	–
E	73.	0.7	11.	0.4	0.5	12.	1.1	–	–

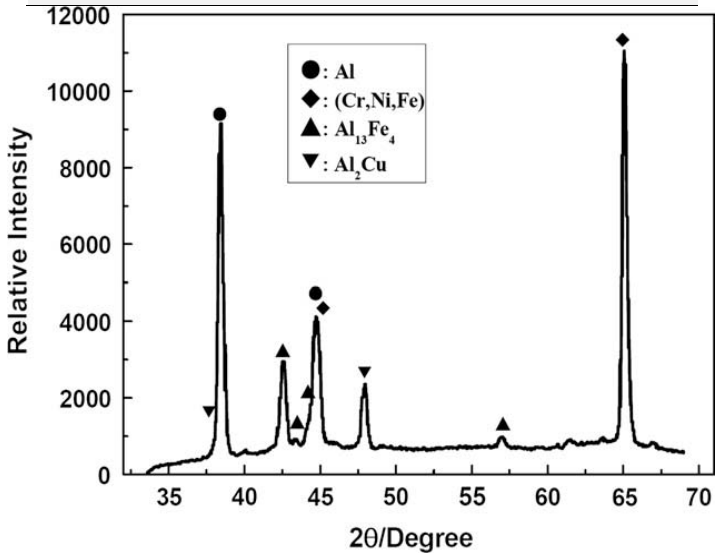

Fig. 5. Micro X-ray diffraction profile of the IMC layer

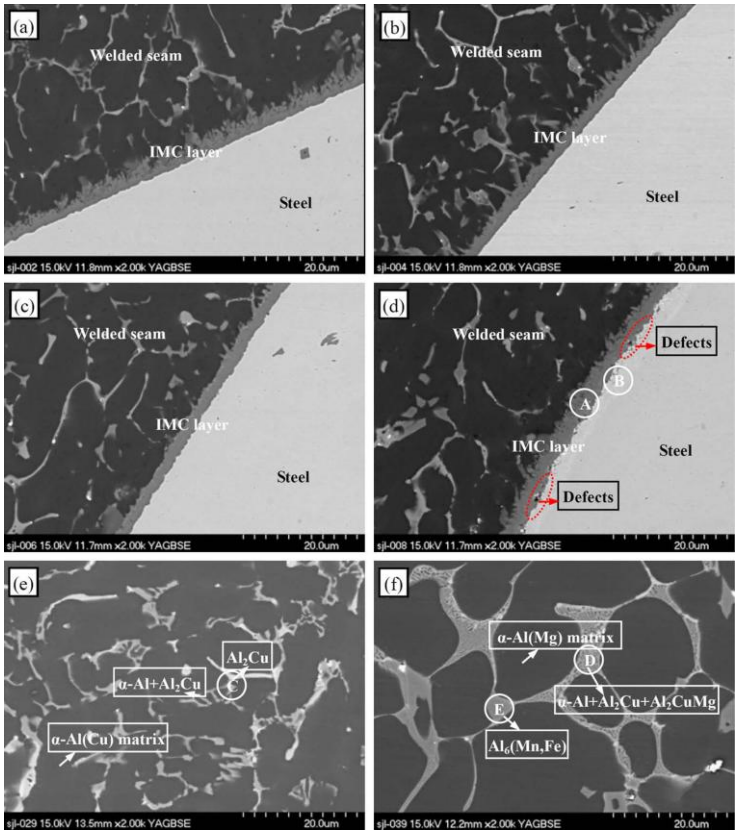

Fig. 4. SEM images in different positions of the aluminum–steel joint in Fig. 3: (a–d) IMC layer in A–D zone, (e) welded seam in E zone, (f) fusion area in F zone.

The EDS analysis compositions of IMCs in the joint, pointed by circles in Fig. 4, are shown in Table 4. The IMC layer has been analyzed to give a composition of 28.3 wt.% Fe and balance Al. At the same time, the layer also contains some contents of Cr, Ni and Cu elements to replace Fe atoms, which enhances the IMC layer's property [15]. Compared the measured composition with the theoretical one of Al–Fe phase [16–18], it is consistent with the composition of $FeAl_3$ or Fe_4Al_{13} phase. At the bottom, the grain boundary filter layer contains about 17.5 wt.% Sn and 3.2 wt.% Zn. In this process, Zn in the flux evaporated due to its low boiling point, while Sn deposited in the molten flux layer due to its high gravity and diffused into the grain boundary of steel matrix.

In welded seam, the composition of the bright phase in grain boundary is 38.5 wt.% Cu and balance Al, which is consistent with the composition of the Al_2Cu phase. The M-XRD profiles of the IMC layer is shown in Fig. 5. The IMC layer is identified as the Fe_4Al_{13} phase and the phase in grain boundary of the welded seam is Al_2Cu. The M-XRD identified results of the IMC layer agree with quantitative one determined by EDS. In fusion area, the network structure in grain boundary is determined to be (α-Al + Al_2Cu + Al_2- CuMg) eutectic phases and the composition of the grey block phase corresponds with $Al_6(Mn,Fe)$.

3.3. Mechanical properties:-

Vicker's hardness of the welded seam and base materials is measured using macro-hardness tester with 10 N loading force and 10 s holding time, and the IMC layer's hardness is measured using dynamic ultra-micro hardness tester with 100 mN loading force and 10 s holding time. The hardness values are shown in Fig. 6. The original hardness of aluminum alloy is 87.4 HV, while in the heat effect zone the average hardness has reduced to 81.4 HV slightly. The softened heat effect zone is weakened due to the lower heat input, which has benefits to the joint property. And in welded seam the average hardness increases to 104.5 HV, due to the strengthening effect of Al_2Cu phase in grain boundary. In the IMC layer, the average hardness increase quickly to 644.7 HV, while it is less than the hardness value 890 HV of standard Fe_4Al_{13} phase. Some contents of Cr, Ni and Cu atoms replacing Fe in Fe_4Al_{13} can

reduce its hardness, which can reduce its brittleness to enhance the IMC layer joining between welded seam and steel.

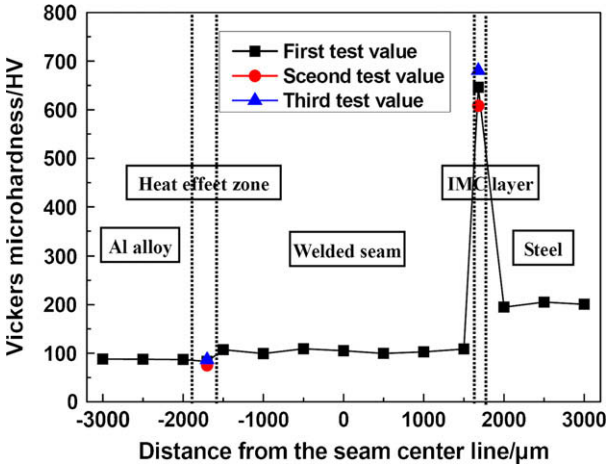

Fig. 6. Hardness distribution of the aluminum–steel joint.

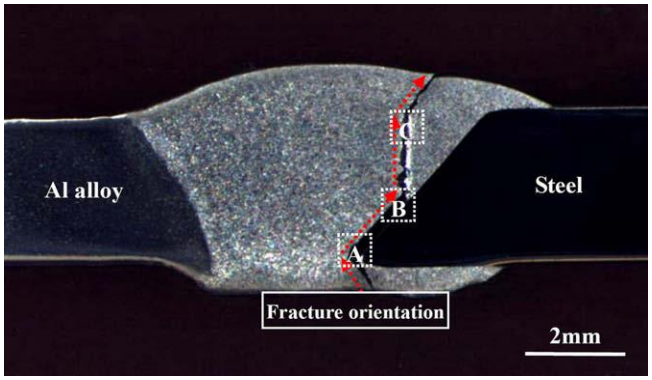

Fig. 7. Macrofracture profile of the aluminum–steel joint.

The tensile strength of the aluminum–steel butt joint using Al– Cu filler metal reaches 172.5 MPa, which is higher than the joint using Al–Si filler metal (about 120 MPa) [6–8]. The macro-fracture profiles of the butt joint is shown in Fig. 7. The crack initiates from the IMC layer at the bottom of the joint and derives into the welded seam at the upper part of the joint, which confirms the IMC layer at the bottom is the weak zone of the joint. The shapes and micro-structures of the IMC layer determine the joint's property. At the bottom, there are some brazing defects between the IMC layer and the grain boundary filter layer, as shown in Fig.5d, which prone to crack at the high load. It has been reported [6] the maximum tensile strength of those butt joint with coated layers was 127.5 MPa and that the fracture occurred at the interface. Hence the present joint using modified non-corrosive flux and Al–Cu filler metal has higher level than those with coated layer.

SEM in situ tensile test was carried out in order to observe the crack growth of the joint during the tensile process. The in situ test results at the different positions of the joint, plotted by dotted-line squares in Fig. 7, are shown in Fig. 8. At the bottom in A zone, the fracture occurs between the IMC layer and steel matrix due to the brazing defects between IMC layer and steel, as shown in Fig. 4d. Upward along the groove, the crack grows between the IMC layer and welded seam and some block IMCs also crack along the front edge of IMC layer in welded seam. Then, at the upper part of the groove, the crack grows in the grain boundary of welded seam duo to Al2Cu phase in grain boundary. The SEM in situ tensile test results agree with the macro-fracture positions in Fig. 7.

III. Conclusions:-

1. Dissimilar metals between 5A06 aluminum alloy and SUS321 stainless steel were butt joined successfully by TIG welding–brazing with Al–Cu filler metal and modified non-corrosive flux.

2. A thin IMC layer has formed in welded seam/steel interface and the average thickness of the whole IMC layer is 3–5 μm, which is less than the limited value of 10μm. The IMC layer consists of Fe_4Al_{13} phase and at the bottom Sn diffuses into steel matrix to form the grain boundary filter layer.
3. The tensile strength of butt- joint reaches 172.5 Mpa and the crack initiates from the IMC layer at the bottom of the joint and derives into the welded seam at the upper part of the joint. The present joint in this study has higher level than those with coated layer.

References:-

[1] Qiu R, Satonaka S, Iwamoto C. Effect of interfacial reaction layer continuity on the tensile strength of resistance spot welded joints between aluminum alloy and steels. Mater Des 2009;30(9):3686–9.

[2] Staubach M, Juttner S, Fussel U, Dietrich M. Joining of steel–aluminium mixed joints with energy-reduced GMA processes and filler materials on an aluminium and zinc basis. Weld Cutting 2008;7(1):30–8.

[3] Acarer M, Demir B. An investigation of mechanical and metallurgical properties of explosive welded aluminum–dual phase steel. Mater Lett

[4] 2008;62(25):4158–60.

[5] Kimura M, Ishii H, Kusaka M, Kaizu K, Fuji A. Joining phenomena and joint strength of friction welded joint between pure aluminium and low carbon steel. Sci Technol Weld Joining 2009;14(5):388–95.

[6] Nezhad M, Ardakani A. A study of joint quality of aluminum and low carbon steel strips by warm rolling. Mater Des 2009;30(4):1103–9.

[7] Achar DRG, Ruge J, Sundaresan S. Metallurgical and mechanical investigations of aluminum–steel fusion welds (1). Aluminium 1980;56(6):391–7.

[8] Song JL, Lin SB, Yang CL, Ma GC, Liu H. Spreading behavior and microstructure characteristics of dissimilar metals TIG welding–brazing of aluminum alloy to stainless steel. Mater Sci Eng A 2009;509(1–2):31–40.

[9] Lin S, Song J, Yang C, Ma G. Microstructure analysis of interfacial layer with tungsten inert gas welding–brazing joint of aluminum alloy/stainless steel. Acta Metall Sin 2009;45(10):1211–6 [in Chinese].

[10] Torkamany MJ, Tahamtan S, Sabbaghzadeh J. Dissimilar welding of carbon steel to 5754 aluminum alloy by Nd:YAG pulsed laser. Mater Des

[11] 2010;31(1):458–65.

[12] Mathieu A, Pontevicci S, Viala JC, Cicala E, Mattei S, Grevey D. Laser brazing of a steel/aluminium assembly with hot filler wire (88% Al, 12% Si). Mater Sci Eng A 2006;435/436:19–28.

[13] Song W, Saida K, Ando A, Nishimoto K. Brazability of aluminum alloy to steels using aluminum filler metal – dissimilar laser brazing of aluminum alloy and steels (Report 1). Quart J Jpn Weld Soc 2004;22(2):315–22 [in Japanese].

[14] Murakami T, Nakata K, Tong H, Ushio M. Dissimilar metal joining of aluminum to steel by MIG arc brazing using flux cored wire. ISIJ Int 2003;43(10):1596–602.

[15] Song JL, Lin SB, Yang CL, Fan CL. Effects of Si additions on intermetallic compound layer of aluminum–steel TIG welding–brazing joint. J Alloys Compd

[16] 2009;488(1):217–22.

[17] Roulin M, Luster JW, Karadenz G, Mortensen A. Strength and structure of furnace-brazed joints between aluminum and stainless steel. Weld J

[18] 1999;78(5):151s–5s.

[19] Qiu R, Iwamoto C, Satonaka S. Interfacial microstructure and strength of steel/ aluminum alloy joints welded by resistance spot welding with cover plate. J Mater Process Technol 2009;209(8):4186–93.

[20] Mekhrabov AO, Akdeniz MV. Effect of ternary alloying elements addition on atomic ordering characteristics of Fe–Al intermetallics. Acta Mater

[21] 1999;47(7):2067–75.

[22] Kawakami Y, Mizoguchi K, Kumai S, Sato A, Kiritani M. Plastic deformation of$Al_{13}Fe_4$ particles in Al–$Al_{13}Fe_4$ by high-speed compression. Mater Sci Eng A

[23] 2003;350(1–2):117–24.

[24] Genba M, Sugiyama K, Hiraga K, Yokoyama Y. Crystalline structure of a Cu- substituted k-$Al_{13}Fe_4$ phase by means of the anomalous X-ray scattering. J Alloys Compd 2002;342(1–2):143–7.